RSC Advances

PAPER

View Article Online
View Journal | View Issue

Cite this: *RSC Adv.*, 2019, **9**, 29312

Sb_2Te_3 as the saturable absorber for the ~2.0 μm passively *Q*-switched solid state pulsed laser

Xihu Wang, *[a] Jinyu Hu,[a] Jinlong Xu,[b] Yijian Sun,[c] Houping Xia[d] and Chaoyang Tu[e]

Received 9th July 2019
Accepted 9th September 2019

DOI: 10.1039/c9ra05209g

rsc.li/rsc-advances

We demonstrated a passively *Q*-switched Tm:YAP solid state pulsed laser based on an Sb_2Te_3 saturable absorber. This saturable absorber was prepared by a facile hydrothermal method. The maximum pulse energy was up to 5.366 μJ at the absorbed pump power of 6.6 W. The corresponding pulse width, output power and repetition rate were 533 ns, 542 mW and 101 kHz, respectively. The results indicated that the hydrothermally synthesized Sb_2Te_3 nanosheet was a promising saturable absorber for near-infrared pulsed lasers.

1. Introduction

To date, Tm^{3+} ($^3F_4 \rightarrow {}^3H_6$) doped pulsed lasers operating around 2.0 μm have attracted much attention owing to their wide applications such as in atmosphere pollution monitoring, eye-safe laser radar, remote sensing, medical treatment and pumping sources for optical parametric oscillators.[1–4] The value of *Q* represents the quality factor of the laser cavity. *Q*-switching technology is a common method to realize pulse lasers. To achieve these lasers, the passively *Q*-switching technology based on a saturable absorber (SA) is a simple method. Transition metal ion doped crystals like Cr:ZnSe and Fe:ZnSe have always been employed as the typical SAs at this waveband, owing to their large absorption cross section and high mechanical stability.[5,6] However, the expensive price and narrow response spectrum limit their development to a certain extent.

Since graphene was successfully used as a SA to produce pulsed lasers,[7] various novel two-dimensional (2D) materials, owing to their advantages of compactness, convenience, and low-cost, have been developed and manifested to be promising saturable absorbers (SAs). For the 2.0 μm waveband, graphene,[8] transitional metal-dichalcogenides (TMDCs),[9] black phosphorus (BP)[10] and topological insulator (TI)[11] are all proved to have the potential to produce pulsed laser. Such materials are formed of groups of atomic layers bound to each other by weak van-der-Waals forces, while in the layers the atoms are strongly bonded by covalent forces.[12] TI, including Bi_2Te_3, Bi_2Se_3 and Sb_2Te_3, stands out from these materials, for its especial band structure. It has conducting states at the surface but behaves like an insulator inside the material, possibly owing to the joining of time-reversal symmetry and spin–orbit interactions.[13] Therefore, it could response for a broadband range benefiting from its surface state, similar to the graphene showing a Dirac-like linear band dispersion.[14] For the other hand, it could enlarge the saturable loss benefitting from its bulk state, compared with graphene. Once discovered, it naturally attracted increasing attention. Until now, many reports have appeared in achieving fiber pulsed laser from 1 to 3 μm.[15–18] Compared with fiber laser, the solid laser was proved to be more suitable for high-energy short pulse generation due to their natures of large mode areas, high thermal conductivity and low undesirable nonlinear pulse-splitting effect. Therefore, it is meaningful to investigate and improve the behavior of TI in the solid state laser.

As a representative of TI, Sb_2Te_3 (ST) has not been explored in the solid pulsed laser so much. Recently, our group firstly applied ST in the solid state laser, achieving a 0.92 μJ pulsed laser at 1045 nm.[19] Then, using the ST thin film prepared by a complicated and expensive pulsed magnetron sputtering method, Loikio *et al.* achieved a 3.5 μJ bulk Tm:$GdVO_4$ pulsed laser at 1905–1921 nm.[20] In this paper, using the ST nanosheets prepared by a facile and cheap hydrothermal method, we obtained a bulk Tm:YAP pulsed laser with a higher pulse energy of 5.366 μJ, and it was meaningful to improve the performance of pulsed laser.

2. Experimental details

Fig. 1 shows the schematic of our laser setup. To compress the volume, we chose a compact plane–plane cavity in this experiment. An a-cut Tm:YAP crystal was used as the gain medium. To

[a]*Key Laboratory of Functional Materials and Devices for Informatics of Anhui Educational Institutions, Department of Physics, Fuyang Normal University, Fuyang, Anhui 236037, China. E-mail: xhwang6@foxmail.com*

[b]*School of Electronic Science and Engineering, Collaborative Innovation Center of Advanced Microstructures, Nanjing University, Nanjing 210093, China*

[c]*School of Metallurgy and Chemical Engineering, Jiangxi University of Science and Technology, Ganzhou, Jiangxi, 341000, China*

[d]*College of Physics and Optoelectronics Technology, Baoji University of Arts and Sciences, Baoji, Shaanxi 721016, PR China*

[e]*Key Laboratory of Optoelectronic Materials Chemistry and Physics of CAS, Fujian Institute of Research on the Structure of Matter, CAS, Fuzhou, Fujian 350002, China*

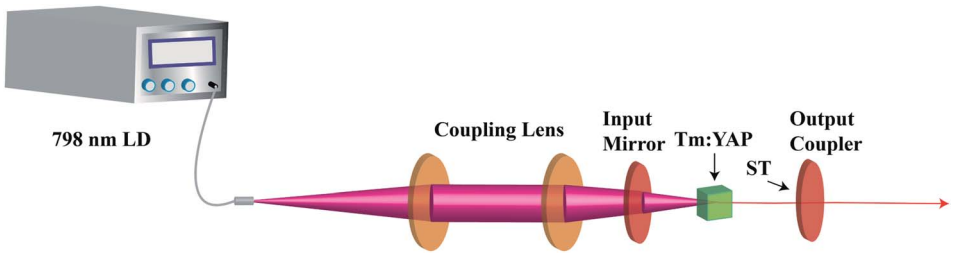

Fig. 1 The schematic of laser setup.

reduce the thermal effects, this crystal was wrapped in indium foil and mounted in a bronze holder cooled with constant 283 K water. The gain medium was end-pumped with a fiber-coupled LD centered at the wavelength of 798 nm. The pump light was then focused in the gain medium with a coupling lens. The input mirror was a plane mirror coated for antireflection at around 798 nm and high-reflection at around 1980 nm. The output coupler was a plane mirror with 3.5% transmittance at 1980 nm. When the *Q*-switching test began, the ST saturable absorber was directly spun onto the output mirror to reduce the insert loss.

A facile hydrothermal method was used to prepare the ST material. This process was described as follow. Firstly, 67.5 mg of $K(SbO)C_4H_4O_6 \cdot 0.5H_2O$, 67.5 mg of $Na_2TeO_3 \cdot 0.5H_2O$ and 450 mg of glucose were dissolved in 5 mL of deionized water. Then, with a constant stirring, 10 mL of ethanediamine was added. After half an hour, this solution was transferred into a 20 mL of Teflon-lined stainless-steel autoclave. It was heated at 180 °C for 12 h and cooled naturally to room temperature. The products were got by sufficient centrifugation and washed with absolute ethanol and deionized water.

3. Results and discussion

The structure feature was explored with an X-ray diffraction (XRD) test and the results are shown as Fig. 2(a). All the diffraction peaks were in good agreement with the crystalline structure of pure ST (JCPDS card no. 15-0874). The lattice plane information was labeled above the corresponding diffraction peak. It indicates that the pure ST material was prepared successfully. To investigate the morphology feature of the products, a scanning electron microscope (SEM) test was selected. Fig. 2(b) shows the corresponding result. From this photo, we could get clearly that a mass of hexagonal sheet-like structures were dispersed randomly. Meanwhile, the sizes of these sheet-like ST were measured one by one. Fig. 2(c) shows the result. The horizontal axis represents the distance between the opposite side of these products and every 50 nm is divided in a unit. The vertical axis represents the corresponding count ratio of these sizes. We could get that the number of the products with the sizes between 400–450 nm is the largest and its count ratio reaches 35.8%. To explore its thickness, the as-prepared ST was also characterized by atomic force microscopy (AFM), as shown in Fig. 3. It had a thickness of about 80 nm and a distance of about 420 nm between the opposite edges. Then the absorption curve was explored. Fig. 4(a) shows the absorption curve at the wavelength range of 1900–2020 nm. We could clearly see that ST possessed a response near 2.0 μm waveband. To explore its nonlinear optics characteristic near 2.0 μm waveband, we employed a home-made acousto-optic *Q*-switched laser, where the Tm:YAP crystal producing 2.0 μm laser was used as the gain medium. The laser power was detected before and after this material, respectively. Fig. 4(b) shows the result. By fitting the curve by the equation

$$T(I) = 1 - \Delta T \times \exp(-I/I_{sat}) - T_{ns}$$

where $T(I)$ is the transmittance, ΔT is the modulation depth, I is the input intensity, I_{sat} is the saturation intensity, T_{ns} is the non-saturable loss, the saturation intensity I_{sat} and the modulation

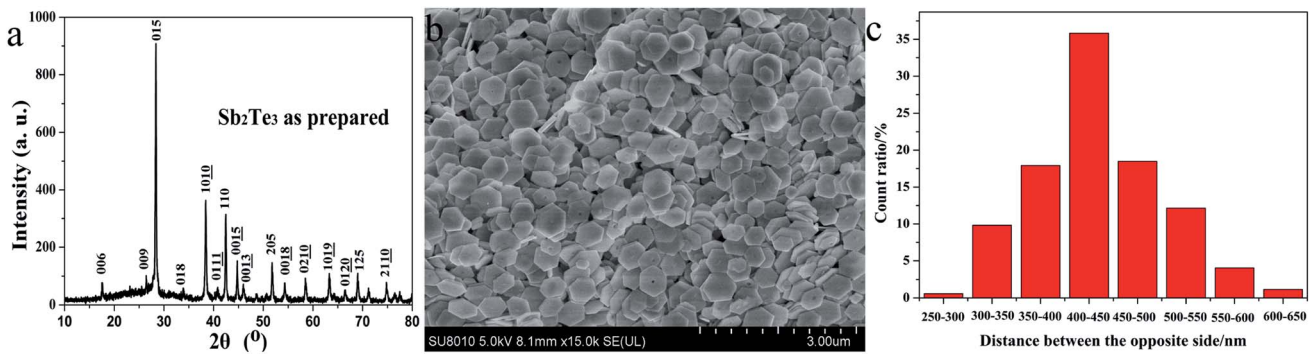

Fig. 2 (a) The XRD pattern, (b) SEM photo and (c) size distribution of the prepared products.

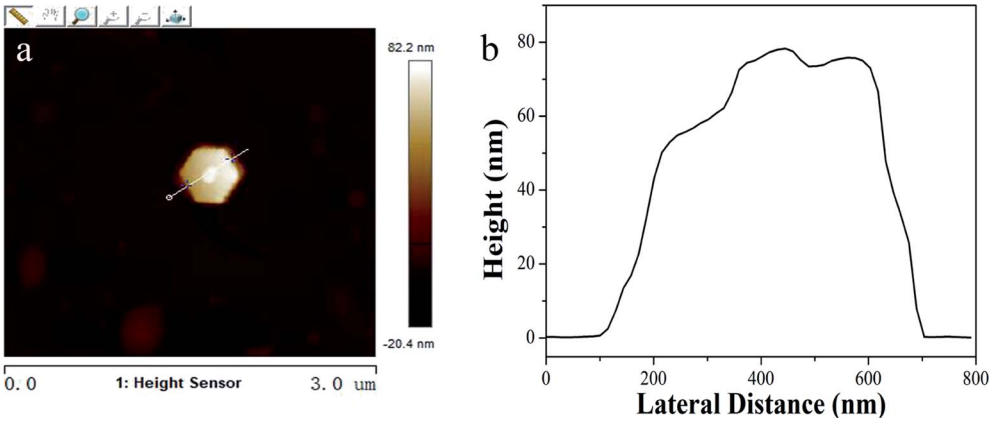

Fig. 3 (a) AFM spectrum and (b) the typical variation of height of the prepared ST.

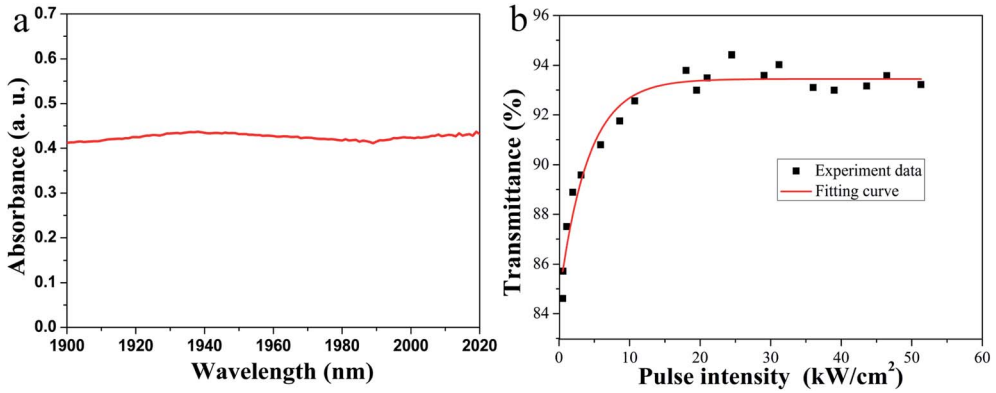

Fig. 4 (a) The wavelength dependence curve and (b) nonlinear absorption curve of ST.

depth ΔT are extracted as 4.10 kW cm^{-2} and 8.80%, respectively. The non-saturable loss is 6.55%.

Firstly, we investigated the continuous laser without the ST saturable absorber. When the absorbed pump power was tuned from the threshold to 5.81 W, no matter how we optimized the cavity, no contiguous stable *Q*-switched pulse train was observed. It indicated that no self *Q*-switching effect during this process. Then about 15 mg of ST powder was dispersed in 5 mL of absolute ethyl alcohol. After an ultrasonic treatment, the dispersion was spun onto the output coupler and it was dried in the air naturally. Then it was tested as follow. With careful adjustment, a series of stable pulse trains began to be observed under 4.25 W of the absorbed pump power. Therefore, the *Q*-switching effect only came from the ST saturable absorber. Then the absorbed pump power was increased successively. When it exceeded 6.6 W, the stable pulse trains started to be unstable. Once decreased, the stable pulse trains appeared again. It indicated the stable *Q*-switched pulse trains could be realized in this section of absorbed pump power and the saturable absorber was not damaged. During this process, the pulse features such as pulse width, repetition rate, output power, pulse energy were also recorded. The corresponding results were shown in Fig. 5(a). At 4.25 W of the absorbed pump power, the pulse width and repetition rate were 920 ns and 60 kHz, respectively. With the increasing of the absorbed pump power, the pulse width decreased continuously and reached the minimum of 533 ns at 6.6 W of the absorbed pump power. In contrast, the repetition rate increased continuously and reached the maximum of 101 kHz. Their relationships were shown in Fig. 5(a). Similarly, the output power increased with the increasing of the absorbed pump power. At the minimum of the absorbed pump power, the output power was the minimum of 226 mW. And at the maximum of the absorbed pump power, it reached the maximum of 542 mW. The relationship between the output power and the absorbed pump power was shown in Fig. 5(b). Based on the data of the repetition rate and output power, we calculated the pulse energy. The largest pulse energy was 5.366 μJ when the absorbed pump power was tuned to 6.6 W. The corresponding result was shown in Fig. 5(b). However, there is a sharp drop of the pulse energy at the absorbed pump power of 6.11 W, and we think it may be caused by the thermal loading. At the maximum of the absorbed pump power, the corresponding pulse trains and single pulse were recorded and Fig. 6(a) and (b) shows the results. Meanwhile, we measured the output laser spectrum and Fig. 6(c) shows the corresponding result. It indicates that the laser operated at 1933–1942 nm. This output spectrum is a typical multiple longitudinal mode output. Because of the high resolution,

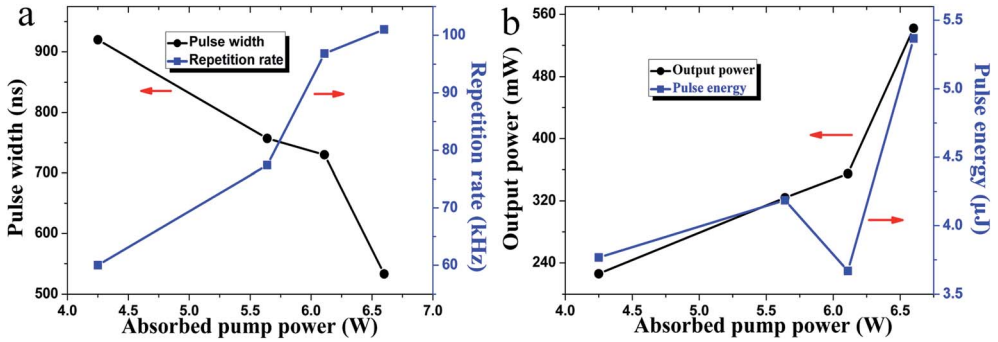

Fig. 5 (a) Pulse width and repetition rate *versus* absorbed pump power, (b) output power and pulse energy *versus* absorbed pump power.

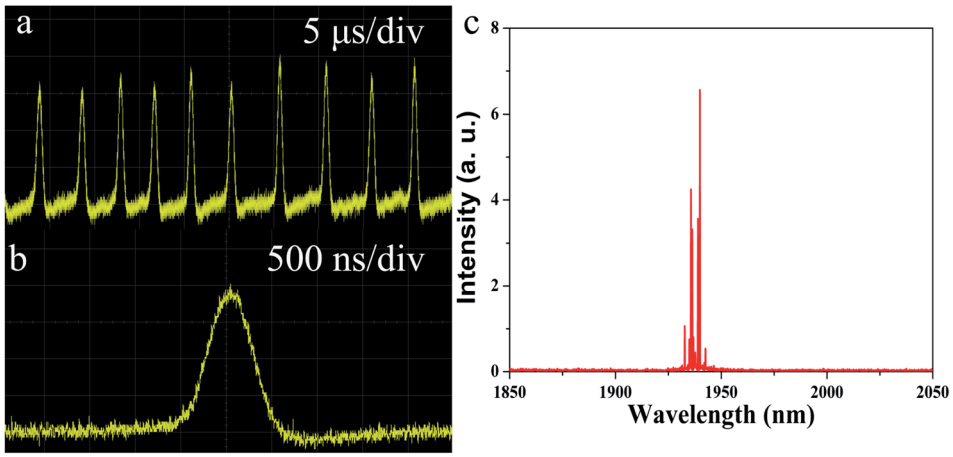

Fig. 6 (a) The pulse trains, (b) single pulse and (c) output spectrum at the absorbed pump power of 6.6 W.

Table 1 Comparison of this 2.0 μm passively *Q*-switched solid-state laser performance with other SAs

Type of SA	Minimum pulse width/ns	Maximum output power/mW	Maximum pulse energy/μJ	Repetition rate/kHz	Gain medium	Ref.
BP	1780	151	7.84	19.25	Tm:YAP	21
MoS_2	435	399	5	55	Tm:YAP	22
Graphene	735	362	8.5	42.4	Tm:YAP	23
ST	533	542	5.366	101	Tm:YAP	This work
MoS_2	800	100	2.08	48.09	Tm:$GdVO_4$	24
Graphene	285	310	1.6	190	Tm:$KLu(WO_4)_2$	25
Gold nanorods	796	380	4.935	77	Tm:YAG	26

many emission lines are distinguished. However, its FWHM is about 5 nm, being consistent with other published data for emission lines of Tm:YAP solid state pulsed laser.[21–23]

To compare this SA with 2.0 μm passively *Q*-switched solid-state laser based on some other nanomaterial SAs, we listed some data like the minimum pulse width, the maximum output power, the maximum pulse energy, the repetition rate and the corresponding gain medium in Table 1. We could clearly get that our results can be considered as superior or at least comparable to the others. To some extent, some shortcomings also existed and our present results could be improved by optimizing the laser cavity, the SA film quality and the thermal loading.

4. Conclusion

Using a facile hydrothermal method, a large quantity of ST nanosheets were obtained with a hexagonal feature. It showed a nonlinear absorption characteristic with modulation depth of 8.8% at 2.0 μm. Based on this SA material, we demonstrated a passively *Q*-switching Tm:YAP solid state pulse laser with the maximum pulse energy up to 5.366 μJ at the absorbed pump power of 6.6 W. The corresponding pulse width, output power and repetition rate were 533 ns, 542 mW and 101 kHz, respectively. Our results indicated that such a material was a promising SA for producing high-performance near-infrared pulsed lasers.

Conflicts of interest

There are no conflicts to declare.

Acknowledgements

This work was supported by the PhD Research Startup Foundation of Fuyang Normal University (2018kyqd0026, 2018kyqd0009), Natural Science Foundation of Jiangxi Province (20181BAB211009), National Natural Science Foundation of China (11804007).

References

1 B. M. Walsh, Review of Tm and Ho materials; spectroscopy and lasers, *Laser Phys.*, 2009, **19**, 855.
2 W. Zeller, L. Naehle, P. Fuchs, F. Gerschuetz, L. Hildebrandt and J. Koeth, DFB Lasers Between 760 nm and 16 μm for Sensing Applications, *Sensors*, 2010, **10**, 2492.
3 V. Wulfmeyer, M. Randall, A. Brewer and R. M. Hardesty, 2-μm Doppler lidar transmitter with high frequency stability and low chirp, *Opt. Lett.*, 2000, **25**, 1228.
4 N. Leindecker, A. Marandi, R. L. Byer, K. L. Vodopyanov, J. Jiang, I. Hartl and P. G. Schunemann, Octave-spanning ultrafast OPO with 2.6–6.1 μm instantaneous bandwidth pumped by femtosecond Tm-fiber laser, *Opt. Express*, 2012, **20**, 7046.
5 B. Cole and L. Goldberg, Highly efficient passively Q-switched Tm:YAP laser using a Cr:ZnS saturable absorber, *Opt. Lett.*, 2017, **42**, 2259.
6 J. Lan, Z. Zhou, X. Guan, B. Xu, H. Xu, Z. Cai and J. Xu, Passively Q-switched Tm:$CaGdAlO_4$ laser using a Cr^{2+}:ZnSe saturable absorber, *Opt. Mater. Express*, 2017, **7**, 1725.
7 Q. Bao, Z. Han, W. Yu, Z. Ni, Y. Yan, Z. X. Shen, K. P. Loh and D. Y. Tang, Atomic-Layer Graphene as a Saturable Absorber for Ultrafast Pulsed Lasers, *Adv. Funct. Mater.*, 2009, **19**, 3077–3083.
8 J. M. Serres, P. Loiko, X. Mateos, K. Yumashev, U. Griebner, V. Petrov and F. Díaz, Tm:$KLu(WO_4)_2$ microchip laser Q-switched by a graphene-based saturable absorber, *Opt. Express*, 2015, **23**, 14108.
9 C. Luan, X. Zhang, K. Yang, J. Zhao, S. Zhao, T. Li and L. Zheng, High-peak power passively Q-switched 2-μm laser with MoS_2 saturable absorber, *IEEE J. Sel. Top. Quantum Electron.*, 2016, **23**, 66.
10 L. Kong, Z. Qin, G. Xie, Z. Guo, H. Zhang, P. Yuan and L. Qian, Black phosphorus as broadband saturable absorber for pulsed lasers from 1 μm to 2.7 μm wavelength, *Laser Phys. Lett.*, 2016, **13**, 045801.
11 X. Liu, K. Yang, S. Zhao, T. Li, W. Qiao, H. Zhang and L. Su, High-power passively Q-switched 2 μm all-solid-state laser based on a Bi_2Te_3 saturable absorber, *Photonics Res.*, 2017, **5**, 461.
12 M. Long, P. Wang, H. Fang and W. Hu, Progress, challenges, and opportunities for 2D material based photodetectors, *Adv. Funct. Mater.*, 2019, **29**, 1803807.
13 J. L. Xu, Y. J. Sun, J. L. He, Y. Wang, Z. J. Zhu, Z. Y. You and C. Y. Tu, Ultrasensitive nonlinear absorption response of large-size topological insulator and application in low-threshold bulk pulsed lasers, *Sci. Rep.*, 2015, **5**, 14856.
14 H. Zhang, C. X. Liu, X. L. Qi, X. Dai, Z. Fang and S. C. Zhang, Topological insulators in Bi_2Se_3, Bi_2Te_3 and Sb_2Te_3 with a single Dirac cone on the surface, *Nat. Phys.*, 2009, **5**, 438.
15 Z. Luo, Y. Huang, J. Weng, H. Cheng, Z. Lin, B. Xu and H. Xu, 1.06 μm Q-switched ytterbium-doped fiber laser using few-layer topological insulator Bi_2Se_3 as a saturable absorber, *Opt. Express*, 2013, **21**, 29516.
16 Z. Luo, C. Liu, Y. Huang, D. Wu, J. Wu, H. Xu and J. Weng, Topological-insulator passively Q-switched double-clad Fiber laser at 2 μm wavelength, *IEEE J. Sel. Top. Quantum Electron.*, 2014, **20**, 1.
17 J. Sotor, G. Sobon, W. Macherzynski and K. M. Abramski, Harmonically mode-locked Er-doped fiber laser based on a Sb_2Te_3 topological insulator saturable absorber, *Laser Phys. Lett.*, 2014, **11**, 055102.
18 G. Jiang, Y. Zhou, L. Wang and Y. Chen, PMMA Sandwiched Bi_2Te_3 Layer as a Saturable Absorber in Mode-Locked Fiber Laser, *Adv. Condens. Matter Phys*, 2018, **12**, 1.
19 X. Wang, J. Xu, Y. Sun, Z. Zhu, Z. You and C. Tu, Near infrared passively Q-switched solid state laser based on Sb_2Te_3 topological insulator saturable absorber, *J. Lumin.*, 2017, **192**, 1.
20 P. Loiko, J. Bogusławski, J. M. Serres, E. Kifle, M. Kowalczyk, X. Mateos and K. Kaszyca, Sb_2Te_3 thin film for the passive Q-switching of a Tm:$GdVO_4$ laser, *Opt. Mater. Express*, 2018, **8**, 1723.
21 Z. Chu, J. Liu, Z. Guo and H. Zhang, 2 μm passively Q-switched laser based on black phosphorus, *Opt. Mater. Express*, 2016, **6**, 2374.
22 C. Luan, X. Zhang, K. Yang, J. Zhao, S. Zhao, T. Li and L. Zheng, High-peak power passively Q-switched 2-μm laser with MoS_2 saturable absorber, *IEEE J. Sel. Top. Quantum Electron.*, 2016, **23**, 66.
23 J. Hou, B. Zhang, J. He, Z. Wang, F. Lou, J. Ning and X. Su, Passively Q-switched 2 μm Tm: YAP laser based on graphene saturable absorber mirror, *Appl. Opt.*, 2014, **53**, 4968.
24 P. Ge, J. Liu, S. Jiang, X. Yu and B. Man, Compact Q-switched 2 μm Tm:$GdVO_4$ laser with MoS_2 absorber, *Photonics Res.*, 2015, **3**, 256.
25 J. M. Serres, P. Loiko, X. Mateos, K. Yumashev, U. Griebner, V. Petrov and F. Díaz, Tm:$KLu(WO_4)_2$ microchip laser Q-switched by a graphene-based saturable absorber, *Opt. Express*, 2015, **23**, 14108.
26 H. Huang, M. Li, P. Liu, L. Jin, W. H. ang and D. Shen, Gold nanorods as the saturable absorber for a diode-pumped nanosecond Q-switched 2 μm solid-state laser, *Opt. Lett.*, 2016, **41**, 2700.

